

ABSTRACT

This study evaluates the air temperature products of Sentinel-3 and Terra MODIS satellite images, with the aim of determining the comparison results of Sentinel-3 and Terra MODIS satellite images for air temperature observations, as well as to determine the minimum and maximum temperatures of the Denpasar area obtained using satellite images. This study took Sentinel-3 and Terra MODIS satellite imagery products with 32 observation samples for the 2021 period and used field observation air temperature data at latitude coordinates $8^{\circ}40'37''$ and longitude coordinates $115^{\circ}12'36''$ at the same time as the satellite image products used in this study. Correlation relationship analysis and Root Mean Square Error (RMSE) were used to investigate the correlation as well as the degree of accuracy between the air temperature of satellite imagery and the air temperature of field observations. The results showed that Sentinel-3 satellite imagery had a correlation of 0.78 to field observation air temperature and RMSE results of 0.93, while Terra MODIS satellite images had a correlation of 0.95 to field observation air temperature and RMSE results of 0.51. Meanwhile, the results of statistical tests show that at the level of $\alpha=0.05$ statistically there is no significant correlation between the air temperature of satellite images (Sentinel-3 and Terra MODIS) and the air temperature of field observations, this is because the P -value > 0.05 . From the results, it was concluded that Terra MODIS satellite images have a better correlation and accuracy level to field observation air temperature compared to Sentinel-3 satellite images with a correlation coefficient comparison difference of 0.17 and an RMSE value comparison difference of 0.42.

Keywords: *Sentinel-3, Terra MODIS, air temperature, RMSE, correlation analysis*

1. INTRODUCTION

An increase in air temperature has a significant relationship with natural conditions, development activities and human life patterns (comfort index) [1]. Related to this, it is necessary to observe and record air temperature periodically. The limited number of meteorological and climatological stations in observing air temperature in the field causes less even air temperature information provided, therefore remote sensing technology is an alternative solution that can be used to observe air temperature evenly for all regions [2]. Remote sensing satellite technology products in the form of satellite images that can be used in the process of observing air temperature are satellite images equipped with electromagnetic wave spectrum

(band) red, near infrared, and thermal infrared [3]. Some satellite images with high temporal resolution and equipped with thermal infrared bands are Sentinel-3 satellite images and Terra Moderate Resolution Imaging Spectroradiometer (MODIS) satellites. In observing air temperature using remote sensing technology (thermal band imagery), the first element that can be identified is surface temperature, therefore the surface temperature obtained by remote sensing systems needs to be converted back to air temperature based on satellite imagery [4]. The results of air temperature observations of each satellite have different levels of accuracy, this level of accuracy is influenced by the bands contained in the satellite and the algorithm used. Therefore, studies on the comparison of Sentinel-3 and Terra MODIS satellite images for air temperature observations need to be studied.

1.2. Sentinel-3 Satellite Imagery

Sentinel satellite imagery is an earth observation satellite of the Copernicus project managed by the European Operational Satellite Agency (EUMETSAT). Until now the Copernicus project continues to grow with a total of 6 Sentinel satellite missions, with different specifications and goals. Sentinel-3 was the third mission of the Copernicus project to launch with 2 types of satellites. The Sentinel-3A satellite was launched on February 16, 2016 and the Sentinel-3B satellite was launched on April 25, 2018. The Sentinel-3 satellite has 4 instruments, namely Sea and Land Surface Temperature Radiometer (SLSTR), Ocean and Land Colour Instrument (OLCI), Sar Radar Altimeter (SRAL) and Microwave Radiometer (MWR) [5]. The Sentinel-3 satellite is designed to monitor sea surface topography as well as land and sea surface temperatures. Of the six projects Copernicus missions underway, only the Sentinel-3 satellite has a thermal infrared band. This infrared thermal band is an important band used in mapping the earth's surface temperature. Sentinel-3 SLSTR satellite imagery, has a low spatial resolution of

500 m to 1 km per 1 pixel, but has several advantages, namely the instruments provided in Sentinel-3 SLSTR, specifically designed for observation of the earth's surface temperature so that Land Surface Temperature (LST) data is available morning and night at the same time. Sentinel-3 SLSTR also has the ability to measure LST with an accuracy level of < 1 K, besides that Sentinel-3 has a high temporal resolution with a revisit time of less than one day at the equator [6]. The Sentinel-3 SLSTR has a medium spectral resolution with 11 bands.

1.3. Terra MODIS Satellite Imagery

Terra MODIS satellite imagery is a National Aeronautics and Space (NASA) mission launched on December 18, 1999 aboard an ATLAS IAS rocket from Vandenberg Air Force Base. Terra satellite is the predecessor satellite of Aqua, Terra satellite has 5 sensors designed to monitor the environment and climate change, the five sensors are Advanced Spaceborne Thermal Emission and Reflection Radiometer (ASTER), Clouds and the Earth's Radiant Energy System (CERES), Multi-angle Imaging Spectro Radiometer (MISR), Moderate-resolution Imaging Spectroradiometer (MODIS) and Measurements of Pollution in the Troposphere (MOPIT) [7]. MODIS is part of the instruments on the Terra satellite that orbits the earth polarly sun-synchronous, the Terra satellite passes from north to south of the equator while the Aqua satellite passes from south to north of the equator [8]. The Terra satellite passed at an altitude of 705 km and crossed the equator in the morning local time, at around 10:30 AM. Terra MODIS satellite has a fairly high temporal resolution product, which ranges from 1 day to 2 days, with a low spatial resolution ranging from 250 m to 1000 m, and has a high spectral resolution with a number of bands that are 36.

1.4. Imagery-Based Air Temperature Analysis

Please note that in remote sensing with thermal band satellite images, the first element that can be identified is surface temperature, so it is necessary to do several stages first to obtain air temperature data. The equation to determine (imagery-based satellite imagery) is as follows:

T_a)

$$T_a = T_s - \left(\frac{H_{raH}}{\rho_{air} C_p} \right) \quad (1)$$

Information:

T_a : Air Temperature (K)

T_s : Surface Temperature (K)

H : Air Heating Flux (Wm^{-2})

ρ_{air} : Air Density ($1,27 \text{ kgm}^{-3}$)

C_p : Specific heat of air at constant pressure ($1004 \text{ Jkg}^{-1}K^{-1}$)

r_{aH} : Aerodynamic resistance (ms^{-1})($31,9u^{-0.96}$)

Aerodynamic resistance is a function of wind speed. The greater the wind speed, the smaller the aerodynamic resistance that inhibits the heat flux [9]. Normal wind speed at a height of 1 m to 2 m is about 2. Wind speed values are differentiated in three land covers: water (2.01 ms^{-1}), non-vegetation (1.79 ms^{-1}) and vegetation (1.41 ms^{-1}). To find the value of H (air heating flux) then used Equation (2.1), Bowen Ratio value, net radiation and soil heat transfer can be seen in Table 1 and Table 2 [10]:

$$H = \frac{\beta (R_n - G)}{1 + \beta} \quad (2)$$

Information:

H : Air Heating Flux (Wm^{-2})

R_n : Net radiation (Wm^{-2})

β : *Bowen ratio*

G : Soil heat transfer (Wm^{-2})

Table 1 *Bowen Ratio* values for each land cover class

No.	Land Closure	Bowen Ratio
1.	Settlement	4,0
2.	Plantation	0,5
3.	Water	0,11
4.	Paddy	0,25
5.	Tropical Forest	0,33

Table 2 R_n and G values of heat transfer for each land cover

No.	Land Cover	R_n	G
1.	Pond	212	15
2.	Rice Fields Vegetation	208	17
3.	Fallow Rice Fields	195	20
4.	Industry	194	21
5.	Urban	194	20
6.	Rural	201	19
7.	Shrub	207	18
8.	Plantation	213	16

2. MATERIALS AND METHODS

This research will be conducted with the selected research location, namely in the Denpasar City area, Bali, which is located at $8^{\circ}40'37''$ LS and $115^{\circ}12'36''$ E, as presented in Figure 1. Data collection and processing will be carried out from March to May 2023.

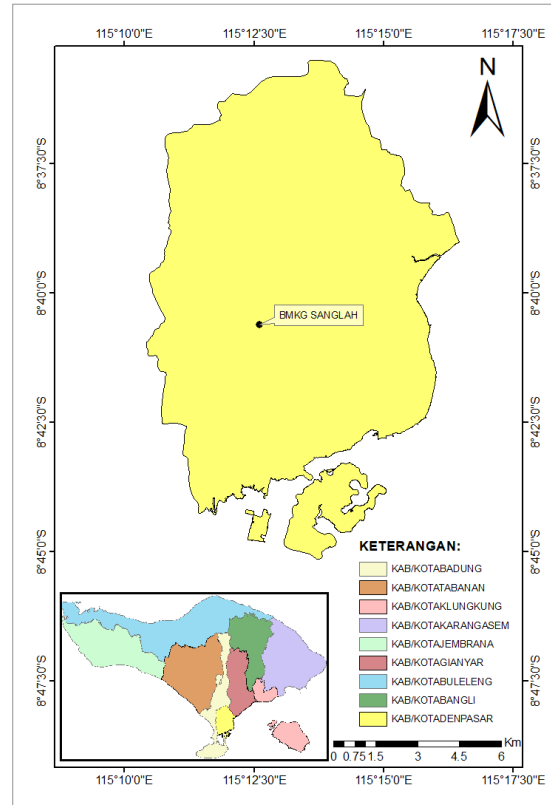


Figure 1 Map of the study area

2.1 Data Collection Methods

The data used in this study are satellite images of the Sentinel-3 SLSTR and Terra MODIS-LST thermal bands, as well as air temperature data from the Meteorology, Climatology and Geophysics Agency (BMKG) Sanglah Geophysical Station Denpasar in 2021. The Sentinel-3 SLSTR satellite image data collection was carried out by downloading directly on the Open Hub Copernicus page <https://scihub.copernicus.eu> and Terra MODIS-LST satellite image data collection by downloading on the United States Geological Survey (USGS) page <https://earthexplorer.usgs.gov/>. The tools used in this study are: Sentinel Application Platform (SNAP), ArcGIS 10.8, Microsoft Excel, and IBM SPSS Statistics.

2.2 Data Processing Methods

Data processing is carried out through several stages, namely, data collection, conversion of Sentinel-3 SLSTR and Terra MODIS-LST satellite images, cutting of research area images, and conversion of ESG on satellite images to air temperature (T_a).

2.3 Data Analysis Methods

The data analysis carried out includes correlation coefficients, T tests, and RMSE. The equation used to determine the value of the correlation coefficient (r) is like Equation (3) which is [11]:

$$r_{x_{\text{sat}}x_{\text{ob}}} = \frac{\sum_{i=1}^n (x_{\text{sat}_i} - \bar{x}_{\text{sat}})(x_{\text{ob}_i} - \bar{x}_{\text{ob}})}{\left(\sum_{i=1}^n (x_{\text{sat}_i} - \bar{x}_{\text{sat}})^2 \sum_{i=1}^n (x_{\text{ob}_i} - \bar{x}_{\text{ob}})^2 \right)^{1/2}} \quad (3)$$

Information:

$r_{x_{\text{sat}}x_{\text{ob}}}$: Correlation coefficient between observation data and satellite data

x_{ob_i} : Observation data in the i -th period with $i = 1, 2, 3, \dots, n$

\bar{x}_{ob} : Average value of observation data

x_{sat_i} : Results of satellite data in the i -th period with $i = 1, 2, 3, \dots, n$

\bar{x}_{sat} : Average value of satellite data results

n : Period length

To facilitate interpretation of the strength of the relationship between the two variables, criteria were created in Table 3 [12].

Table 3 Parameters of correlation coefficient

Parameters	Category
$r = 0$	There is no correlation between the two variables
$0 < r \leq 0.25$	The positive correlation is very weak
$0.25 < r \leq 0.50$	The positive correlation is quite weak
$0.50 < r \leq 0.75$	Strong positive correlation
$0.75 < r \leq 0.99$	The positive correlation is very strong
$r = 1$	Perfect positive correlation
$0 \geq r > -0.25$	The negative correlation is very weak
$-0.25 \geq r > -0.50$	The negative correlation is quite weak
$-0.50 \geq r > -0.75$	Strong negative correlation
$-0.75 \geq r > -0.99$	The negative correlation is very strong
$r = -1$	Perfect negative correlation

2.3.1. T-Test

In this study the T-test was used to determine the significance of the correlation coefficient statistically, researchers used an error significance level (*alpha*) of 5% (0.05) and with a confidence degree of 95%. In performing the T-test, the hypotheses formulated for each independent variable are as follows:

1. Sentinel-3 satellite image with BMKG air temperature

$H_0: \rho_{sb} = 0$, then there is no significant correlation between Sentinel-3 satellite images and BMKG air temperature.

$H_1: \rho_{sb} \neq 0$, there is a significant correlation between Sentinel-3 satellite images and BMKG air temperature.

2. Terra MODIS satellite image with BMKG air temperature

$H_0: \rho_{tb} = 0$, then there is no significant correlation between Terra MODIS satellite images and BMKG air temperature.

$H_1: \rho_{tb} \neq 0$, then there is a significant correlation between the Sentinel-3 satellite image and BMKG air temperature.

Acceptance or rejection of this hypothesis test is carried out with the following criteria:

- a. If the P Value $> \alpha$ (0.05) then H_0 is accepted and H_1 is rejected (Insignificant).
- b. If the P Value $< \alpha$ (0.05) then H_1 is accepted and H_0 rejected (Significant).

2.3.2 RMSE calculation

RMSE is a large rate of error in prediction results, where the smaller the RMSE value (close to zero), the better or more accurate the RMSE value will be. The RMSE value can be calculated using Equation (4) [11].

$$\text{RMSE} = \sqrt{\frac{\sum_{i=1}^n (x_{\text{ob}_i} - x_{\text{sat}_i})^2}{n}} \quad (4)$$

Information:

x_{ob_i} : Observation data in the i -th period with $i = 1, 2, 3, \dots, n$

x_{sat_i} : Results of satellite data in the i -th period with $i = 1, 2, 3, \dots, n$

n : Amount of data

To determine the category of accuracy obtained from RMSE, RMSE value parameters are used. The RMSE value parameters can be seen in Table 4 [13].

Table 4 RMSE value parameters

Parameters	Accuracy Rate Categories
$RMSE \leq 0.75$	Excellent
$0.75 < RMSE \leq 1$	Good
$1 < RMSE \leq 2$	Enough
$RMSE > 2$	Not Accurate Enough

2.4 Framework of Thought

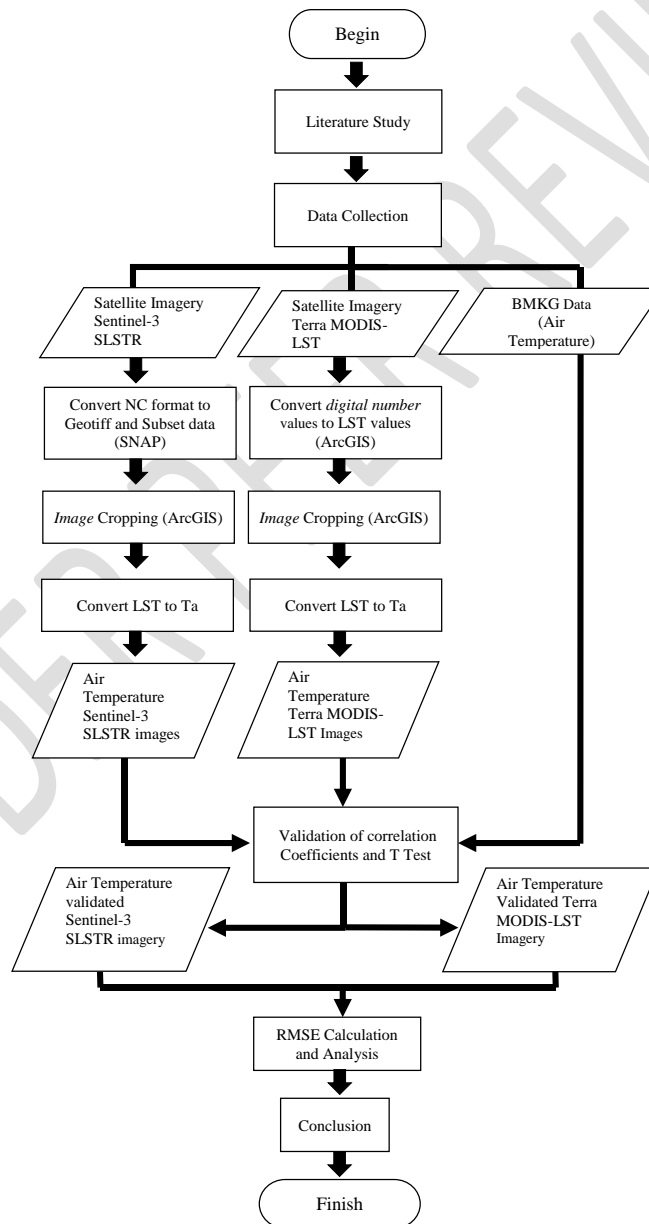


Figure 2. Frame of Mind

3. RESULTS AND DISCUSSION

3.1. Air Temperature Measurement Results of Sentinel-3 Satellite Image

Based on the processing that has been carried out, there were 32 observation times for the 2021 period in the Denpasar area with at least <10% cloud cover. By using satellite images, it can be known which areas have minimum and maximum temperatures in the Denpasar area, besides that on the same observation the Denpasar area has different air temperatures. Based on the results, it is known that in 32 observations of the 2021 period in the Denpasar area, the minimum temperature that can be detected by Sentinel-3 satellite images was 9.51°C on September 23, 2021 in the South Denpasar area, and the maximum temperature was 41.50°C on April 14, 2021 in the West Denpasar area. In addition to knowing the minimum and maximum temperatures, air temperatures at the point of the research location have also been obtained, then graphs can be formed, namely the Sentinel-3 air temperature pattern graph with BMKG air temperature (Figure 3) and regression charts (Figure 4). Figure 3 shows that the Sentinel-3 air temperature pattern graph almost follows the BMKG air temperature pattern chart, but it can be seen that there is an air temperature difference that causes the Sentinel-3 air temperature chart pattern to tend to be higher than the BMKG air temperature chart pattern. The largest difference in air temperature between the air temperature of the Sentinel-3 satellite image and the air temperature of BMKG was found on July 19, 2021, with a difference of 2.63. In Figure 4 is shown a graph of points between Sentinel-3 air temperature and BMKG air temperature, it can be seen that the points in the graph spread irregularly around the diagonal line. From the regression graph, it is also known that the value of the coefficient of determination is 0.6038, which means that the BMKG air temperature that can be explained by the Sentinel-3 air temperature is 60.38%.

Through the results of the calculation of the correlation coefficient and t test, it can be seen that the air temperature of the Sentinel-3 satellite image with BMKG air temperature has a correlation coefficient value of 0.78 which in Table 3, the value of the correlation coefficient is included in the very strong positive correlation category ($0.75 < r < 0.99$). In the t-test results, it was found that in the air temperature of the Sentinel-3 satellite image with BMKG air temperature, the population correlation coefficient was statistically insignificant. This is because the resulting P value is greater than the α value ($0.42 > \alpha (0.05)$), so $H_0: \rho_{sb} = 0$ is accepted. This means that the correlation between the air temperature of the Sentinel-3 satellite image and the air temperature of the BMKG is not significant (statistically there is no significant correlation). Insignificant t-test results can be due to the small number of samples, this statement is supported by Nurminen's (1997) research which says that in large population groups, even small differences become statistically significant, while in small samples, clinically significant observations can remain statistically insignificant [14]. The insignificant t-test results in this study are also supported by Xiong and Chen's (2017) research [15], with similar topics regarding temperature observations of Landsat satellite images and field observations that also produce statistically insignificant correlations.

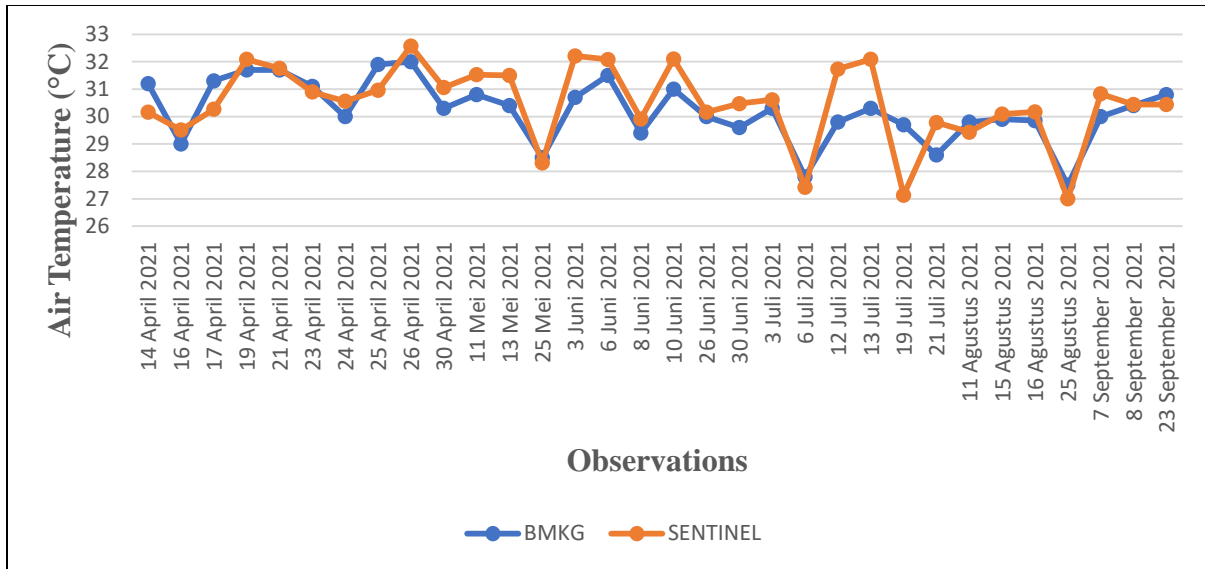


Figure 3 Sentinel-3 air temperature pattern with BMKG air temperature

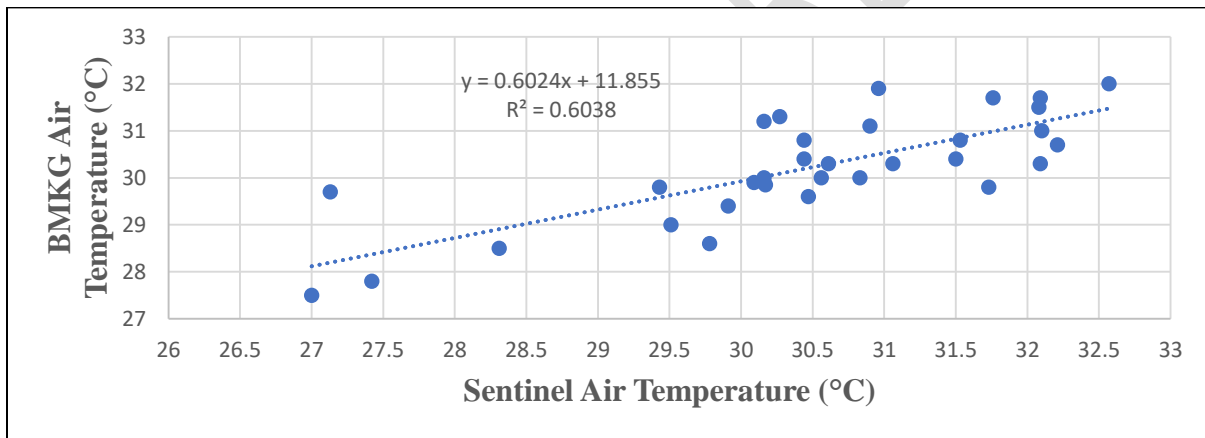


Figure 4 Regression graph of Sentinel-3 air temperature with BMKG air temperature

3.2 Air Temperature Measurement Results Terra MODIS Satellite Image

From the processing results, it is known that in 32 observations of the 2021 period in the Denpasar area, the minimum temperature that can be detected by Terra MODIS satellite images was 20.57°C on September 23, 2021 in the South Denpasar area, and the maximum temperature was 37.08°C on April 16, 2021 in the West Denpasar area. In addition to knowing the minimum and maximum temperatures, the air temperature at the point of the research location has also

been obtained. Figure 5 shows that the Terra MODIS air temperature pattern graph almost follows the BMKG air temperature pattern graph, the largest air temperature difference between the air temperature of Terra MODIS satellite images and BMKG air temperature is found on April 14, 2021, with a difference of 1.17. In Figure 6 is shown a graph of points between Terra MODIS air temperature and BMKG air temperature, it can be seen that the points in the graph spread irregularly around the diagonal line. From the regression graph, it is also known that the value of the coefficient of determination is 0.895, which means that the BMKG air temperature that can be explained by the Sentinel-3 air temperature is 89.50%.

Through the results of the calculation of the correlation coefficient and t test, it can be seen that the air temperature of the Terra MODIS satellite image with BMKG air temperature has a correlation coefficient value of 0.95 which in Table 3, the value of the correlation coefficient is included in the very strong positive correlation category ($0.95 < r < 0.99$). In the t-test results, it was found that in the air temperature of the Terra MODIS satellite image with the BMKG air temperature, the population correlation coefficient was statistically insignificant. This is because the resulting P value is greater than the α value ($0.15 > \alpha (0.05)$), so $H_0: \rho_{tb} = 0$ is accepted. This means that the correlation between the air temperature of Terra MODIS satellite imagery and BMKG air temperature is not significant (statistically there is no significant correlation relationship). The difference in minimum and maximum air temperatures obtained by each satellite image can be caused by atmospheric disturbances such as cloud cover or differences in spectral resolution owned by Sentinel-3 and Terra MODIS. This is supported by Cervest's (2020) article [16] and in Wang et al's (2023) research [17] which says that the higher the spectral resolution, the better the ability of satellite image sensors to identify wavelengths.

Terra MODIS has a very narrow bandwidth, so it can better distinguish subtle differences in surface reflections, and can better predict temperature.

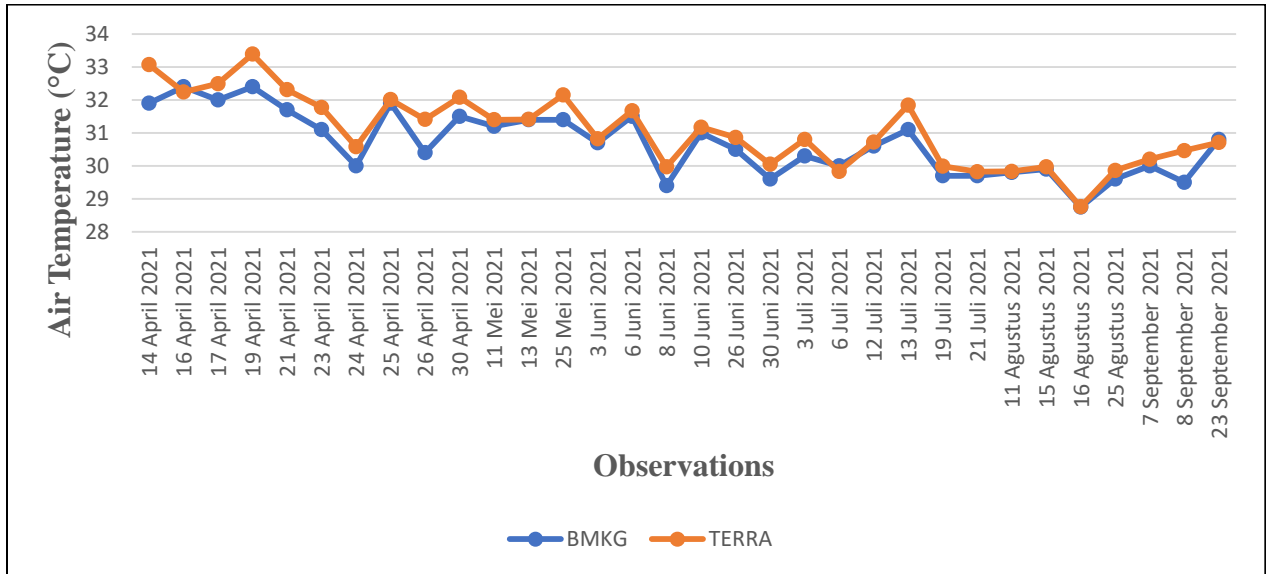


Figure 5 Terra MODIS air temperature pattern with BMKG air temperature

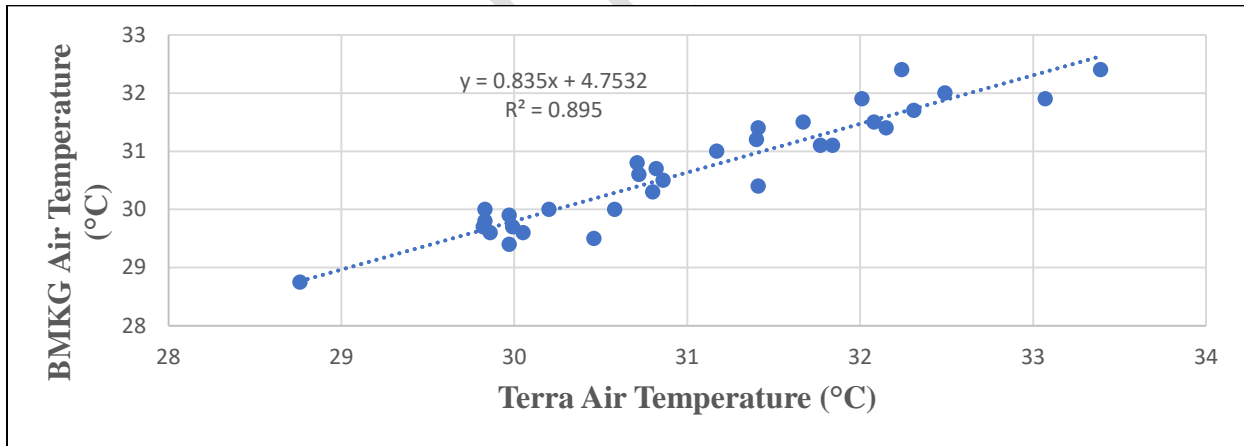


Figure 6 Terra MODIS air temperature regression graph with BMKG air temperature

3.3 Results of Correlation Coefficient Calculation and Statistical Testing t

After the air temperature on the Sentinel-3 and Terra MODIS satellite images was successfully obtained, then validation and data analysis were carried out using correlation

coefficient calculations and statistical tests t. The results of the calculation of the correlation coefficient and statistical testing t can be seen in Table 5 and Table 6.

Table 5 Results of correlation coefficient calculation

No.	Variable	r value	Category r	Value r ²
1.	Sentinel-3 with BMKG	0,78	Positive is very strong	0,60
2.	Terra MODIS with BMKG	0,95	Positive is very strong	0,89

Table 6 Statistical test results t

No.	Variable	P Value	Interpretation	Information
1.	Sentinel-3 with BMKG	0,42	$0.42 > \alpha (0.05)$	Insignificant
2.	Terra MODIS with BMKG	0,15	$0.15 > \alpha (0.05)$	Insignificant

3.4. RMSE Calculation Results

The RMSE calculation is performed using Equation 4. The RMSE calculation results can be seen in Table 7.

Table 7 RMSE Results

No.	Variable	RMSE value	Accuracy Rate Categories
1.	Sentinel-3 with BMKG	0,93	Good Accuracy Rate
2.	Terra MODIS with BMKG	0,51	Excellent Accuracy Rate

4. CONCLUSION

Based on the analysis that has been done, it can be concluded that:

1. The minimum temperature detected by Sentinel-3 satellite images from 32 observations was 9.51°C on 23 September 2021 and the maximum temperature was 41.50°C on 14 April 2021. Meanwhile, in Terra MODIS satellite images from 32 observations, the

minimum temperature was 20.57°C on September 23, 2021 and the maximum temperature was 37.08 on April 16, 2021.

2. Terra MODIS satellite imagery has a better correlation and accuracy rate to BMKG air temperature compared to Sentinel-3 satellite imagery. The difference in the correlation coefficient of Terra MODIS satellite imagery with Sentinel-3 is 0.17 and the difference in the comparison of RMSE values is 0.42. Through the difference in correlation comparison and the level of accuracy obtained, the error in the Sentinel-3 satellite image in air temperature observations is greater than the error in the Terra Modis satellite image. So it can be noted that Terra MODIS satellite images are better used in air temperature observations than Sentinel-3 satellite images.

REFERENCE

1. Alfiandy, S., Imron, A.R., and Donald, S.P. 2022. Air Temperature Increase Pattern Based on BMKG and ERA5 Data in Central Sulawesi Province. *Journal of Forest Policy Analysis*. 19(1): 63-70
2. Hooker, J., Gregory, D., and Alessandro, C. 2018. A Global Dataset of Air Temperature Derived from Satellite Remote Sensing and Weather Stations. *Scientific Data*. 5(180246): 1-11
3. Faisal, A., Indarto., Elida, N., and Budiyono. 2018. Utilization of Satellite Imagery to Generate Air Temperature Information to Support Water Resources Management. *National Seminar in the framework of the 42nd Anniversary*.
4. Runke, W., Xiaoni, Y., Yaya, S., Chengyong, W., and Baokang, L. 2022. Study on Air Temperature Estimation and Its Influencing Factors in A Complex Mountainous Area. *PLOS ONE*. 17(8): 1-23
5. The European Space Agency. 2022. *Sentinel Online*. <https://sentinels.copernicus.eu/web/sentinel/missions/sentinel-3>. Retrieved January 19, 2023.
6. Mirnayani., Sry, K.R., Andi, N.A., and Atar, A.B. 2021. Utilization of Sentinel-3 Sea and Land Surface Temperature Radiometer (SLSTR) Morning and Night Image Data for Analysis of the Intensity of the Bahang Surface Island Phenomenon (Case Study: Bandung City). *Journal of Remote Sensing and Digital Image Data Processing*. 18(1): 15-25

7. Satrioajie, W.N. 2012. MODIS satellite imagery technology for sea surface temperature measurement. *Oceana*. 37(3): 1-9
8. Handayani, T, and Desyanti. 2019. Compression of Fashionable Terra Satellite Imagery using Shortwave Switching. *SATIN-Science and Information Technology*. 5(2): 1-8
9. Desi. 2011. Application of Remote Sensing to Estimate Surface and Air Temperatures in Peatlands and Minerals Using Energy Balance Method (Study Area: Sampit, Central Kalimantan). Department of Geophysics and Meteorology. Bogor Agricultural University. *Thesis*
10. Wiweka. 2014. Surface and Air Temperature Patterns Using Multitemporal Landsat Satellite Imagery. *Ecolab Journal*. 8(1): 1-52
11. Natadiredja, S. 2018. Daily Rainfall Validation Based on Global Satellite Mapping of Precipitation (GSMAP) Data in Bali and Nusa Tenggara Regions. Faculty of Mathematics and Natural Sciences. Udayana University. *Thesis*
12. Ahemaitihali, A, and Zouji, D. 2022. Spatiotemporal Characteristics Analysis and Driving Forces Assessment of Flash Floods in Altay. *Water*. 4(331): 2-18
13. Schermelleh, K.E., and Helfried, M. 2003. Evaluating the Fit of Structural Equation Models: Tests of Significance and Descriptive Goodness of Fit Measures. *Methods of Psychological Research Online*. 8(2): 23-74
14. Nurminen, M. 1997. Statistical Significance - A Misconstrued Notion in Medical Reseach. *Scand J Work Environ Health*. 23(2): 232-235
15. Xiong, Y., and Chen, F. 2017. Correlations Analysis between Temperatures from Landsat Thermal Infrared Retrievals and Synchronous Weather Observations in Shenzhen, China. *Remote Sensing Applications: Society and Environment*. 7: 40-48
16. Cervest. 2020. Remote Sensing of Planet Earth – Part 3: Fashionable vs Sentinel-2. <https://cervest.earth/>. Retrieved June 2, 2023
17. Wang, S., Feng, Y., Fu, D., Kong, L., Li, H., Han, B., and Lu, F. 2023. Stratospheric Temperature Observations by Narrow Bands Ultra-High Spectral Resolution Sounder from Nadir-Viewing Satellites. *Remote Sens*. 15(1967)